Functional characterization of 29D09 effectors from the potato cyst nematode *Globodera rostochiensis*

A Thesis

Presented to the Faculty of the Graduate School

of Cornell University

In Partial Fulfillment of the Requirements for the Degree of

Master of Science

by

Yi-Chun Yeh

May 2021

ABSTRACT

Plant-parasitic cyst nematodes penetrate root tissues of host plants and secrete effector proteins into host cells to establish successful parasitism. The Gr29D09 effector family from the potato cyst nematode *Globodera rostochiensis* is exclusively expressed in the nematode's dorsal gland cell and is comprised of at least 27 variants. Constitutive expression of one of these variants, *Gr29D09-V3,* in potato has previously been shown to increase susceptibility to both *G. rostochiensis* and common scab (*Streptomyces scabies*). In this thesis, five representative Gr29D09 variants, V1, V3, A2, F10 and OA3, were selected for functional characterization. Plant immunity assays performed in *Nicotiana benthamiana* showed that all five variants suppressed flg22-triggered ROS production as well as the hypersensitive response (HR) induced by Gpa2/RBP-1 and Rx/CP. A co-immunoprecipitation-coupled with nanoLC-MS/MS approach identified mitochondria-associated StHXK7 as a specific interactor with Gr29D09-V3, a result confirmed with bimolecular fluorescence complementation assays. Elevated levels of *StHXK7* mRNA were observed both in *G. rostochiensis*-infected potato roots and in transgenic potato plants expressing *Gr29D09-V3*. Localization of *StHXK7* expression with a

StHXK7promoter:GUS reporter line further revealed that *StHXK7* was upregulated at the nematode-feeding site and its surrounding tissue. Lastly, StHXK7 was found to inhibit flg22-triggered ROS production in *N. benthamiana*. These data collectively support a model in which Gr29D09-V3 suppresses flg22-triggered ROS production through enhancing accumulation of *StHXK7* mRNA and/or physically interacting with and stabilizing StHXK7 on mitochondria of plant cells.

BIOGRAPHICAL SKETCH

Yi-Chun Yeh (Athena) grew up in Taiwan. She obtained her Bachelor of Science degree in Life Science at National Taiwan University in 2006 and Master of Science degree in Molecular and Cellular Biology at National Taiwan University in 2008. She continued her education at Cornell University in the Biochemistry, Molecular and Cellular Biology program in 2011. In 2016 summer, she transferred to Dr. Xiaohong Wang's lab in Plant Pathology and Plant-Microbe Biology at Cornell University. After a one year health leave in 2019, she returned to Cornell to complete her master's degree.

ACKNOWLEDGMENTS

I would like to thank my advisor, Dr. Xiaohong Wang, for learning in her laboratory. This provided a connection between my original background in basic science and real world problems in agriculture. She also provided me chances to present the work at difference conferences. These were good opportunities to enhance my oral presentation skills and interact with researchers outside Cornell. I would like to thank my committee members, Drs. Walter De Jong and Gregory Martin for their advice and support on different aspects.

I would like to thank people in Dr. Wang's lab. Shiyan Chen taught me the skills and shared materials required for the research in this thesis. Her experience sharing helped me troubleshoot. She helped generate the *StHXK7promoter:GUS* construct during my health leave. Thanks to Huijun Yang for maintaining *N. benthamiana* plants and preparing *G. rostochiensis* cysts for my experiments. Thanks to Joshua Kwan for assisting with agroinfiltration. Thanks to Mingkee Achom for supporting each other as office mates.

TABLE OF CONTENTS

CHAPTER 1: INTRODUCTION

Plant-parasitic cyst nematodes, *Heterodera* and *Globodera* spp., are sedentary biotrophic pathogens of many crops of economic importance (Chitwood, 2003; Jones et al., 2013). In the soil, these microscopic worms hatch from eggs inside cysts as motile second-stage juveniles (J2). Attracted by signals from host roots, J2s move towards and penetrate host roots near the root tip (Gheysen and Mitchum, 2011). They migrate intracellularly and select a cell near the vasculature as an initial syncytial cell, which is then transformed into a syncytium, a large metabolically active structure with multiple nuclei (Gheysen and Mitchum, 2011). The syncytium serves as a nutrient sink to support nematode growth and subsequent development into adult males and females (Fig. 1.1A).

To successfully cause disease, plant pathogens secrete effectors, either proteins or small molecules into host cells (Hogenhout et al., 2009). Effectors perturb the host cellular machinery in various ways to benefit the pathogen (Fig. 1.1A). Cyst nematodes secrete effector proteins that are primarily produced from esophageal glands (two subventral glands and one dorsal gland) into host plant cells through their stylet (Fig. 1.1B). Genes encoding these effectors show distinct

temporal expression profiles as the nematode establishes a parasitic relationship with the host (Mitchum et al., 2013; Thorpe et al., 2014). The two subventral glands enlarge with rich secretory granules in the pre-parasitic J2 stage (Hussey and Mims, 1991; Mitchum et al., 2013). The effectors generated in the two subventral gland cells mainly function during the early stage of nematode infection and include cell wall modifying enzymes to facilitate nematode migration within the root tissue (Smant et al., 1998; Cotton et al., 2014; Akker et al., 2017). In contrast, the size and activity of dorsal gland cell increases in nematode parasitic stages (Hussey, 1989). RNAseq expression profiling of effector genes from *G. pallida* substantiated effectors produced in the dorsal gland cell are expressed and secreted into host cells during nematode parasitic stages (Thorpe et al., 2014). These effectors serve many functions, such as suppressing plant defenses, altering specific developmental pathways of the host, and initiating and maintaining the formation of the syncytium (Vieira and Gleason, 2019). Understanding how cyst nematode effectors function may help guide the development of novel management strategies.

(A) (B)

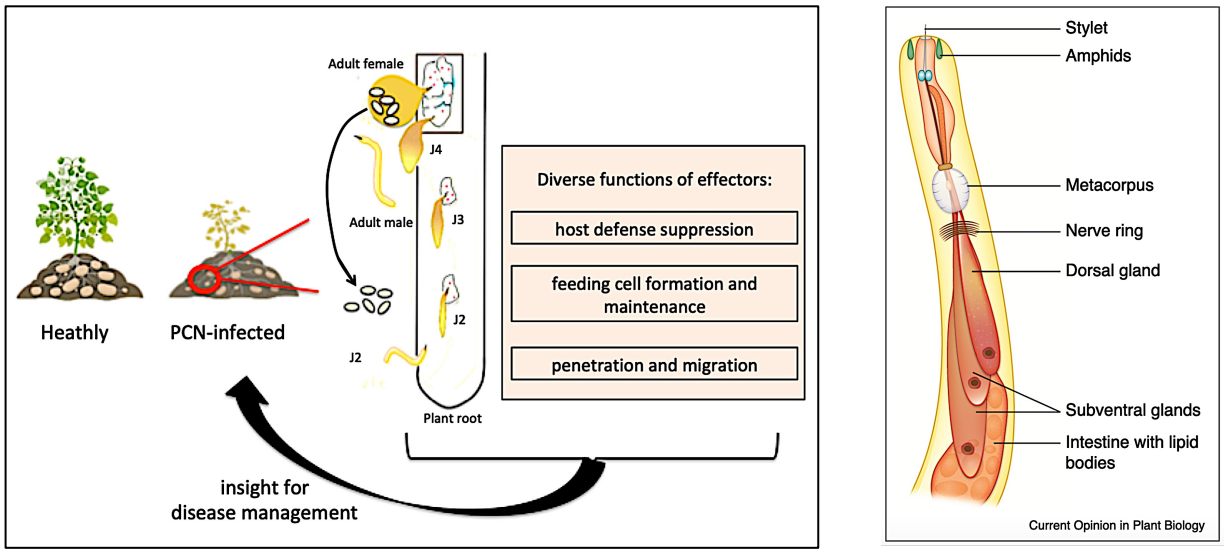

Fig. 1.1 PCNs are major pathogens of potatoes. (A) PCNs secrete different effectors to facilitate infection and parasitism of potato plants. Understanding how effectors work can provide insight for integrated disease management. (B) The esophageal gland cells, major sites that produce effectors, in the anterior part of a plant parasitic nematode in the J2 stage (adapted from Current Opinion in Plant Biology 2019, 50:37–43).

Plants have evolved an innate immune system to fend off the attacks of microbial pathogens. The classic zigzag model provides a summary of the dynamic evolutionary arms race between host and pathogen (Jones and Dangl, 2006). In the first branch of the plant immune system, pattern recognition receptors (PRRs) on the host plant cell surface detect conserved pathogen-associated or microbe-associated molecular patterns (PAMPs or MAMPs) from

pathogenic microbes. This leads to a host response in the form of pattern-triggered immunity (PTI), which includes a burst of reactive oxygen species (ROS), callose deposition and the elevated expression of defense-related genes (Saijo et al., 2018; Luna et al., 2011). Some virulence effectors from pathogens defeat PTI and cause effector-triggered susceptibility (ETS) (Jones and Dangl, 2006). The second branch of the plant immune system recognizes pathogen effectors with resistance (R) proteins and results in localized cell death, referred to as a hypersensitive response (HR), which limits the spread of the pathogen (Heath, 2000). This is known as effector-triggered immunity (ETI). Studies have shown that these two branches share common signaling components downstream, such as the influx of Ca^{2+} and the contribution of RbohD in ROS production have been found in both PTI and ETI (Peng et al., 2018; Lu and Tsuda, 2021).

The novel gene *29D09* has previously been identified in the soybean cyst nematode *H. glycines* and has been hypothesized to encode for an effector protein (Gao et al., 2007; Thorpe et al., 2014; Yang et al., 2019). However, the molecular function of Hg29D09 is unknown. To clone the orthologous gene in *G. rostochensis*, our lab designed primers based on the gene

identified in *G. pallida* (Jones et al., 2009) and performed RACE-PCR on *G. rostochensis* cDNA. The lab identified a total of 27 variants in the *Gr29D09* family. Five variants were selected as representatives for further functional investigation in this thesis: V1, V3, A2, F10 and OA3 (Fig. 1.2). Each member of the *Gr29D09* gene family encodes a putative protein with less than 200 amino acids (V1: 198; V3: 198; A2: 189; F10: 194; OA3: 155) with an N-terminal signal peptide of 24 amino acids for secretion. Excluding the N-terminal signal peptide yields a cytoplasmic version of Gr29D09 variants that can be used for functional studies *in planta*, including this thesis. Variants of the Gr29D09 protein share 76-89% sequence identity with Gp29D09 and 51-54% with Hg29D09. Homologs of *29D09* have only been found to date in cyst nematodes, suggesting that this gene is specific to cyst nematodes and might have arisen as a result of an evolutionary arms race between cyst nematodes and their hosts.

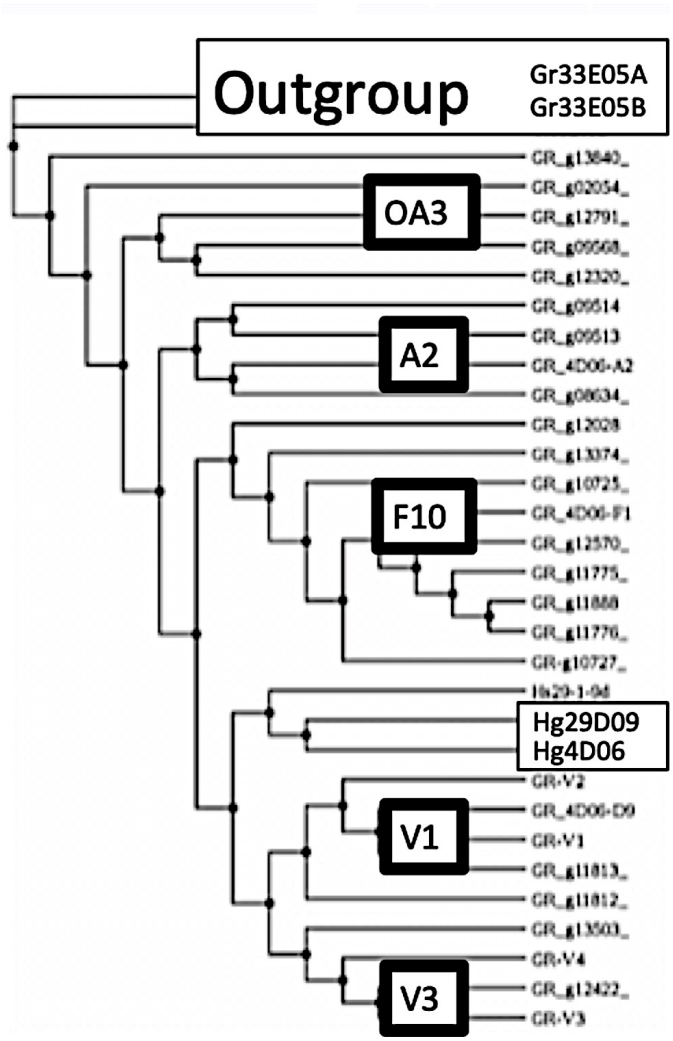

Fig. 1.2. A phylogenetic tree of the Gr29D09 gene family. V1, V3, A2, F10 and OA3 were selected as representative variants for functional studies in this thesis.

The spatial and temporal expression of *Gr29D09* provided initial clues that this gene family might promote nematode parasitism. *In situ* hybridization revealed that *Gr29D09* transcripts are expressed exclusively in the dorsal gland cell of nematode parasitic stages. In terms of timing, *Gr29D09* was found to be upregulated upon the onset of parasitism; expression

peaked at late parasitic J2 (par-J2) stage and then gradually reduced at later parasitic stages. Fluorescence microscopy has shown that Gr29D09:GFP fusion protein localizes to the cytoplasm of the host plant cell when *Gr29D09:GFP* was transiently expressed in *Nicotiana benthamiana* (X. Wang Lab, unpublished results).

To test whether Gr29D09 plays an important role in *G. rostochiensis* infection, transgenic potato lines expressing $Gr^{\Delta SP}$*29D09-V1* or $Gr^{\Delta SP}$*29D09-V3* were generated and tested for nematode infection. All transgenic lines with high levels of *29D09* expression showed increased susceptibility to *G. rostochiensis* infection (X. Wang Lab, unpublished results). The results suggest a role of 29D09 effectors in plant defense suppression.

To further evaluate a role of Gr29D09 effectors in host defense suppression, I conducted PTI and ETI assays in a heterologous system, *N. benthamiana*, described in this thesis. The five Gr29D09 variants suppress PTI at different levels, with V3 showing the most suppression ability. All five Gr29D09 variants also suppress RBP1/Gpa2 and Rx/CP-induced HR in an ETI assay, with A2 exhibiting the strongest suppression activity. These results imply that Gr29D09 variants have evolved to target different components of plant defense pathways.

Our lab has also previously searched for potato proteins that physically interact with Gr29D09-V3 using nanoLC-MS/MS analysis. Potato Hexokinase7 (StHXK7) was identified this way and further confirmed as a host target of Gr29D09-V3 with a pull-down assay and a bimolecular fluorescence complementation (BiFC) assay. I discovered that StHXK7 is mitochondria-associated and the interaction between StHXK7 and Gr29D09-V3 was located on mitochondria. With RT-qPCR, I found it difficult to detect the expression of *StHXK7* in non-infected potato roots. Nematode infection, though, increased its expression level considerably. Additionally, elevated mRNA of *StHXK7* was found in transgenic potato lines with *Gr29D09-V3* overexpression when compared to wild-type potatoes. GUS staining of *StHXK7promoter:GUS* lines revealed that *StHXK7* is specifically upregulated at and surrounding nematode infection sites. Further characterization of StHXK7 demonstrated that it can suppress PTI. All these data lend to a model that during nematode infection, Gr29D09-V3 interferes with plant defense by suppressing ROS production by enhancing the expression of *StHXK7* mRNA and/or physicallly interacting with StHXK7, with the latter possibly serving to stabilize StHXK7 on mitochondria.

CHAPTER 2: MATERIALS AND METHODS

DNA constructs

For functional assays, the Gr29D09 variants A2 and F10 without signal peptide were amplified from plasmids pGEMT-A2 and pGEMT-F10 with primer pairs (Gr4D06A2XbaIDSPF and Gr4D06A2BamHIR) and (Gr4D06F10XbaIDSPF and Gr4D06F10BamHIR), respectively (Table 2.1), and then cloned into a pMD1 vector in between a 35S promoter at the 5′ end and an HA tag at the 3′ end. The Gr29D09 variant OA3 was amplified directly from cDNA prepared from *G. rostochiensis*-infected roots collected at 7-15 days post-inoculation (dpi) and was also cloned into an HA-tagged pMD1 expression vector. Expression constructs of *Gr29D09-V1* and *Gr29D09-V3* have previously been described (Tran, 2016). Construction of *StHXK7p:GUS* is described further below.

Table 2.1. Primers used in this study

Primer	Primer sequence (5′-3′)	Application
For cloning *Gr29D09* variants		
Gr4D06A2XbaIDSPF	CCAATCTAGACCAACCATGGCCCCACAATT	Clone A2 into pMD1 vector
Gr4D06A2BamHIR	GGTTGGATCCTCAGAGCTTGTGCGAGCCGG	Clone A2 into pMD1 vector
Gr4D06F10XbaIDSPF	CCAATCTAGACCAACCATGGCGCCCAGTTT	Clone F10 into pMD1 vector
Gr4D06F10BamHIR	GGTTGGATCCTTATTGTTTTGTGTAAGCGC	Clone F10 into pMD1 vector
XbaI-Gr9568-dSP	TACATCGTTCTAGAATGCCACAATTCCCGT GCTGTGCCGGCAG	Clone OA3 from nematode-infected root cDNA
BamHI-Gr9568-dSTOP-R	GAGTTTGTGTGAGCCGGATTCGCCTGGGAT CCATGCATGC	Clone OA3 from nematode-infected root cDNA
For measuring expression level of *StHXK7*		
StHxk7-143bp-f	GTAAGACTCAAGATGCAAAGC	RT-qPCR
StHxk7-300bp-r	CAATGCATAAAAGACGCCAG	RT-qPCR
StRPN7-F	TTGGGGTGTCTGAGGATTTC	Housekeeping gene as internal control
StRPN7-R	CATTCTTTGCATCAGGACGA	Housekeeping gene as internal control
For *StHXK7promoter:GUS* cloning		
StHx7pro_BamHI-4R	GAAGGATCCTTTTTGCCGGAATTTGAGGT	Amplify promoter region for promoter driven GUS construct
StHx7pro_SalI-2368F	GAGGTCGACGCAACAGTTTGCTATGGGGT A	Amplify promoter region for promoter driven GUS construct

ROS assay

To detect the ROS burst, an established luminol-HRP based protocol (Segonzac et al., 2011) was used. Three-week-old *N. benthamiana* plants were moved from the greenhouse to a growth chamber (20 to 25°C, 35-50% humidity and 16 hr:8 hr light-dark cycle) one day before the start of the assay. Eight plants were used for one ROS assay. pMD1 expression vector with tag only and AvrPtoB (Kim et al., 2002, Lindeberg et al., 2012) were used as negative and positive controls, respectively. *Agrobacterium tumefaciens* strain GV3101 carrying these expression constructs were introduced into well-expanded leaves via agroinfiltration. Leaf discs were harvested with a cork borer (4 mm diameter) 48 hours after infiltration and the discs were then placed, adaxial side up, into a well of a 96-well microplate filled with 200 µl of water for 16-24 hours. The water was then replaced with 100 µl of assay solution (17 mM luminol, 1 µM horseradish peroxidase and 100 nM flg22). The production of ROS was monitored for 45 min using a microplate reader (Segonzac et al., 2011). *Gr29D09* variants and *StHXK7* were all tested at least two times. Each time, every gene was run in triplicate with three leaf discs from an infiltration spot. A t-test was used to analyze differences between maximum relative

luminescence units.

ETI assay

Two pairs of resistance (*R*) genes and their associated effector (now referred to as Avirulence or *Avr*) genes were used to induce the hypersensitive response (HR) in leaves of *N. benthamiana*: Gpa2/RBP–1 (Sacco et al., 2009) and Rx2/CP (Bendahmane et al., 2000). HA-tagged Gr29D09 variants without a signal peptide were used in this assay. The pMD1 vector with HA-tag only and a construct expressing *GrCEP12:HA* (Chen et al., 2013) were included as negative and positive controls, respectively. Constructs were transformed into *A. tumefaciens* GV3101 for agroinfiltration into leaves of four to five-week-old *N. benthamiana* plants. Briefly, *A. tumefaciens* was grown at 28°C on a solid medium with selective antibiotics overnight. Cells were collected, resuspended in infiltration medium, and adjusted to a final optical density$_{600}$ (OD_{600}) of 0.3. For two R/Avr pairs, each *A. tumefaciens* (Sacco et al., 2009) was prepared with OD_{600} of 0.3. Cells from R and Avr were then combined with equal volume to reach the final OD_{600} of 0.15. Two days after Gr29D09 variants were introduced into leaves, R/Avr pairs were infiltrated at the same sites. HR phenotype development was then monitored up to five days. The

infiltrated site was categorized as exhibiting an HR phenotype when cell death represented ≥ 75% of the infiltrated area. HR suppression ability of each Gr29D09 variant was compared to GrCEP12 (which suppresses HR) and HA (which does not suppress HR). At least three independent experiments were conducted for each R/Avr pair.

Nematode infection

Potato plants were propagated from tissue culture stocks. Nodal cuttings were cultivated on solid propagation medium with timentin (Chronis et al., 2014a). Plantlets were grown in an incubator with 16h/8h light/dark cycle at 22°C. Eleven to 13 day-old plantlets were used for nematode infection with an established protocol (Lu et al., 2008; Chronis et al., 2014a). Briefly, *G. rostochiensis* pathotype Ro1 was maintained on susceptible potato (*Solanum tuberosum* cv. Katahdin) in the greenhouse. The cysts were extracted from soil and soaked in distilled water for five days. The eggs were then released from the cysts by crushing and incubated in potato root diffusate with Gentamycin and Nystatin antibiotics for the hatching of preparasitic second-stage juveniles (pre-J2s). Pre-J2s were surfaced sterilized as described previously and used for inoculation (Chronis et al., 2014a). Each plant was inoculated with 200-400 pre-J2s. Infected

plantlets were maintained in the dark at 20°C and infection status of roots was monitored with a dissecting microscope. Roots containing nematodes at different developmental stages (e.g., parasitic J2, J3, J4 stages) were collected at various time points after inoculation. Uninoculated roots were used as a control. Root samples prepared for gene expression analyses were stored in a −80°C freezer until needed, while root samples prepared for checking promoter activity of *StHXK7promoter:GUS* potato lines were immediately subjected to the GUS staining protocol described below.

RT-qPCR

To study the expression profile of *StHXK7* during nematode infection and in a *Gr29D09-V3* overexpression potato line, mRNA was extracted from nematode-infected roots with the Dynabeads mRNA DIRECT Kit (Invitrogen, Carlsbad, CA) and cDNA was then synthesized to serve as template for quantitative PCR (qPCR) (Lu et al., 2008). 1.3-1.5 μg cDNA was added in a 25 μl reaction solution containing iQ SYBR Green Supermix (Bio-Rad Laboratories, Hercules, CA). For forward and reverse primers, 150 nM was used for StHXK7 and 500 nM was used for the potato *RPN7* gene, which was an endogenous reference for qPCR.

qPCR was performed in an iCycler iQ Real-Time PCR Detection System (Bio-Rad Laboratories, Hercules, CA). PCR cycling conditions were 95 ° C for 3 min of DNA denaturation, then followed by 40 cycles of 95°C for 20s and 60°C for 40s. Every RT-qPCR contained three technical replicates of each cDNA sample. The expression levels were calculated with the comparative cycle threshold (C_t) ($2^{-\Delta\Delta Ct}$) method (Lu et al., 2009).

Generating *StHXK7promoter:GUS* lines

To generate the *StHXK7promoter:GUS* construct, a 2368 bp sequence upstream of *StHXK7* was amplified from genomic DNA of potato 'Désirée' using primers StHx7pro_BamHI-4R and StHx7pro_SalI-2368F (Table 2.1) and cloned into the binary vector pBI101.2 at the *Sal*I and *Bam*HI restriction sites. Transgenic potato plants expressing *StHXK7promoter:GUS* were generated using an established lab protocol (Chronis et al., 2014b). Briefly, potato nodal stem segments were first cultivated on propagation medium in a growth incubator with a 16 h/8 h light/dark cycle at 24°C for four to six weeks. The internodal stem sections were then excised and transferred to CIM plates for *Agrobacterium* transformation. *A. tumefaciens* strain LBA4404 carrying the *StHXK7p::GUS* construct was collected from liquid

culture with OD_{600} of 0.7. The transformed segments were placed on solid 3C5ZR medium with proper antibiotics for selection until shoots emerged. The plantlets were then transferred to propagation medium with appropriate antibiotics. The transgenic potato lines were confirmed by PCR screening of genomic DNA extracted from plantlets' leaves.

GUS staining

Line 6 of transgenic potato expressing *StHXK7p:GUS* was grown and subjected to nematode infection as described above. At various time points roots from infected and non-infected plants were collected and vacuum infiltrated with GUS substrate buffer (100 mM Tris, pH 7, 50 mM NaCl,1 mM 5-bromo-4-chloro-3-indolyl-b-glucuronic acid, 0.06% [v/v] Triton X-100) and incubated for two days at 37°C (Jefferson et al., 1987). To stain nematode juveniles, GUS-stained roots were incubated in 1% (v/v) hypochlorite for 7 min, then rinsed thoroughly in tap water for 20 min. These roots were then boiled in acid fuchsine solution (118 mM acid fuchsine and 0.5% [v/v] acetic acid) for 1 min and left in the staining solution for an additional 30 min. The stained roots were rinsed with and stored in 100% Ethanol. A Nikon Eclipse TS100 inverted microscope was used to observe if there was blue GUS staining at the

nematode infection sites in stained roots. To examine the spatial expression profile of *StHXK7* during normal plant growth, transgenic line 6 was grown in a glass tube. The GUS staining protocol here was applied to the whole plant once roots and shoots had emerged.

Western blotting

N. benthamiana leaves in PTI and ETI assays were collected after 2 days of agroinfiltration. The leaves were homogenized in extraction buffer (50 mM HEPES-KOH pH 7.5, 150 mM NaCl, 0.5% Triton X-100, 1% Tween 20, 1% Protease cocktail (Sigma Aldrich), 0.5% PMSF) and filtered through a disposable sample filter column (Fisher cat# 11-387-50). 2 X SDS sample buffer (Bio-Rad Laboratories) with 5% β-mercaptoethanol was added into protein samples heated for 10 min at 95°C. Proteins were resolved by SDS-PAGE and subsequently transferred onto on nitrocellulose membrane (Bio–Rad Laboratories). After blocking with PBS (80 mM Tris/HCl, pH 7.5 and 137 mM NaCl, 2.7 mM KCl, 10 mM Na_2HPO_4, 1.8mM KH_2PO_4) containing 5% w/v nonfat dry milk overnight at 4°C, the membrane was incubated with anti-HA antibody (1:4000 dilution) at room temperature for 2 hr. Bands were visualized with HRP substrate (Millipore, Billerica, MA) following exposure using MultiImage Light Cabinet Filter Positions (Alpha Innotech Corporation).

CHAPTER 3: RESULTS

Gr29D09 effectors suppress plant PTI response

Prior results in our lab suggested a role of the *Gr29D09* effector gene family in host defense suppression. Namely, *Gr29D09* genes are highly upregulated in nematode parasitic stages and, in pathogen infection assays, the ectopic expression in potato of either of two *Gr20D09* variants, $Gr^{\Delta SP}$*29D09-V1* or $Gr^{\Delta SP}$*29D09-V3,* increased susceptibility to both *G. rostochiensis* and the unrelated soil pathogen *S. scabies* (X. Wang Lab unpublished results). In this study I sought to understand how Gr29D09 suppresses host defense. There are 27 variants in the *Gr29D09* gene family. To facilitate the functional study, Gr29D09 variants OA3, A2, F10, V1, and V3 were selected as representative members of different clades of the phylogenetic tree (Fig. 1.2). All five were examined to see if they have a role in suppressing PTI and/or ETI.

A burst of ROS is one of the early PTI responses (Boller and Felix, 2009). I used a luminol-based assay (Keppler et al., 1989; Chen et al., 2013) to measure ROS accumulation after treatment with flg22, a well-studied PAMP of bacterial pathogens, in *N. benthamiana*. With this assay, five representative Gr29D09 variants with HA tag were evaluated for their abilities to

suppress a flg22-induced ROS burst in *N. benthamiana*. The known PTI suppressor AvrPtoB from *Pseudomonas syringae* DC3000 (Kim et al., 2002, Lindeberg et al., 2012) and a vector with an HA tag were included as positive and negative controls, respectively. On a scale of 0 to 100, the luminol signal of the HA tag-only vector was set to 100, against which all remaining signals were normalized. The positive control AvrPtoB suppressed 98% of ROS production (Fig. 3.1A). As Gr29D09-V1, V3, A2 and F10 showed similar protein expression levels based on Western blots (Fig. 3.1B), the ROS suppression ability of these four variants can be compared quantitatively. The Gr29D09-OA3 variant, on the other hand, was expressed at a lower level (data not shown), and will be discussed qualitatively. All five Gr29D09 variants suppressed ROS production significantly when compared to the HA-tag only control (Fig. 3.1A). As these five representatives covered ancestral and present variants in the phylogenetic tree and (Fig. 1.2) it might suggest that all members of the Gr29D09 gene family have the ability to suppress ROS production. Among Gr29D09-V1, V3, A2 and F10, V3 reduced ROS production most strongly, up to 51%, while the remaining variants, V1, A2 and F10 suppressed up to 23%, 31% and 20% respectively (Fig. 3.1). Collectively, these results suggest that Gr29D09 variants have a role in

PTI suppression.

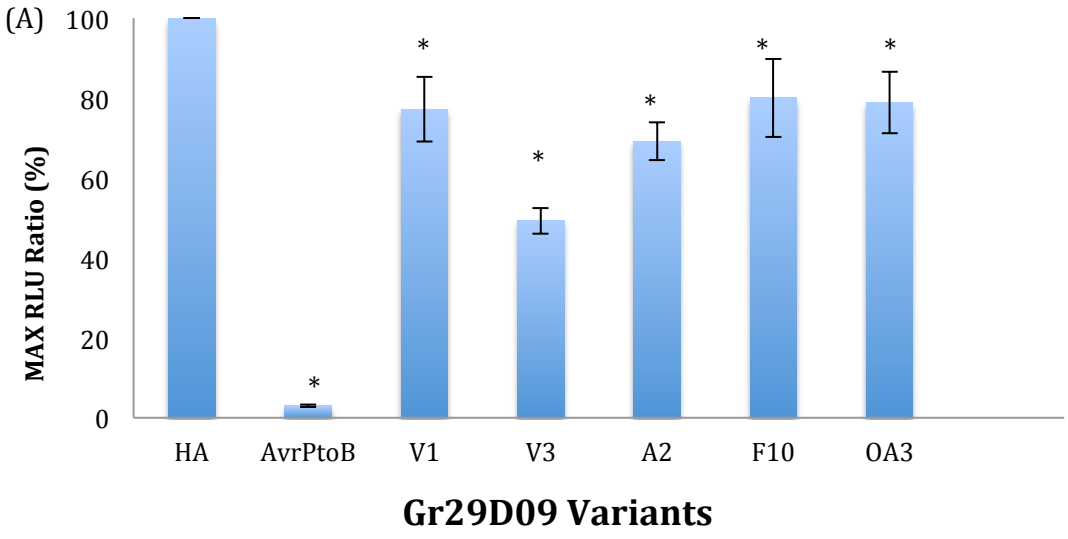

Fig. 3.1 Gr29D09 variants suppress flg22-triggered ROS production in *N. benthamiana*. *Agrobacterium tumefaciens* strain GV3101 carrying HA, AvrPtoB, HA tagged Gr29D09 variants (V1, V3, A2, F10, and OA3) expression constructs were separately infiltrated into leaves of 3-week-old *N. benthamiana* plants. Infiltrated leaf discs were collected 48 h post-agroinfiltration and assayed for ROS production. The analysis of Gr29D09 variants were repeated at least three times (V1: 4, V3: 6, A2: 7, F10: 4, OA3: 3 times individually) and similar results were obtained each time. Y-axis values indicate maximum relative luminescence units (MAX RLUs) with at least 26 leaf discs per variant (V1: 33, V3: 35, A2: 39, F10: 33, OA3: 26 discs separately). Error bars represent the mean ±SD. Significant

differences between HA and variants are indicated by an asterisk (Student's t-test at $P < 0.05$). (B) Protein expression level of Gr29D09 variants in infiltrated *N. benthamiana* leaves. The leaf discs were collected 48 h after of agroinfiltration and subjected to Western Blotting.

Gr29D09 effectors suppress HR cell death mediated by different plant R proteins

To test whether 29D09 effectors could also suppress ETI, they were analyzed for ability to suppress the hypersensitive response (HR) in a heterologous *N. benthamiana* system (Chronis et al., 2013). Each of the five Gr29D09 variants was agroinfiltrated into leaves of *N. benthamiana*. Two days later, a plant R gene (*Gpa2* or *Rx*) and its cognate pathogen avirulence effector (*RBP-1* or *CP*, respectively) were co-infiltrated at the same sites to induce cell death (Sacco et al., 2009; Bendahmane et al., 2000). Over the following five days, the development of an HR phenotype on leaves was monitored to determine whether any of the Gr29D09 variants interfere with ETI signaling *in planta*. Vectors expressing HA-tag and GrCEP12 were used as negative and positive controls, respectively, on every agroinfiltrated leaf (Chronis et al., 2013). If the area of cell death comprised 75% or more of an agroinfiltrated spot, it was categorized as an HR response; if less than 75%, HR was deemed as suppressed. The co-expression of *Gpa2/RBP-1* or *Rx/CP* elicited HR at infiltration spots expressing HA-tag (Fig. 3.2). All five Gr29D09 variants suppressed HR induced by Gpa2/RBP-1 and Rx/CP significantly when compared to the HA-tag only control (Fig. 3.2). The protein expression levels of Gr29D09-V1, V3, A2 and F10 were again similar,

while Gr29D09-OA3 accumulated to lower levels (western blot data not shown). In the ETI assay with Gpa2/RBP-1, Gr29D09 variants V1, V3, A2 and F10 suppressed HR significantly at 69%, 64%, 79% and 71% of infiltrated sites when compared to the HA-tag vector control respectively. In Rx/CP-induced HR experiments, Gr29D09 variants V1, V3, A2 and F10 significantly suppressed HR at 65%, 58%, 79% and 51% respectively when compared to HA-tag vector control. Overall, Gr29D09-A2 exhibited the strongest ability to suppress HR, 79% for both Gpa2/RBP-1 and Rx/CP-induced HR.

That all five Gr29D09 variants suppressed both PTI and ETI suggests that they may function redundantly in suppressing host defenses. Among Gr29D09 variants V1, V3, A2 and F10, Gr29D09-V3 suppressed ROS production the best and Gr29D09-A2 performed best in inhibiting the development of defense-related cell death. These observations suggested that Gr29D09 effectors might have evolved with different functions and that they might target distinct host proteins to interfere with and dampen plant immunity.

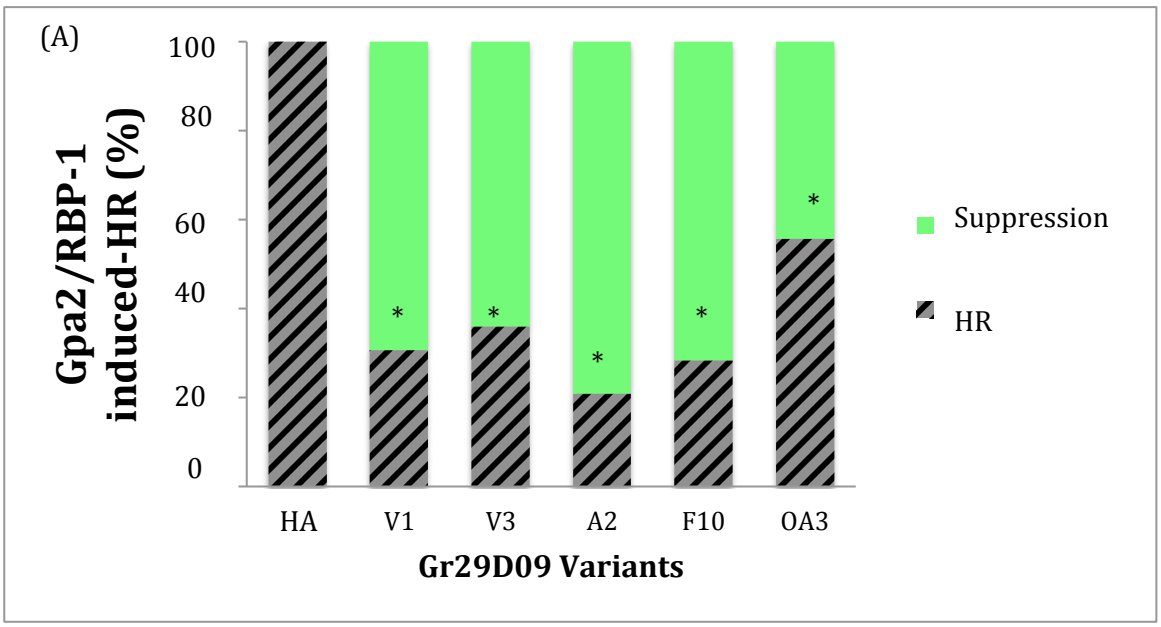
(A)
Gpa2/RBP-1 induced-HR (%)
100
80
60
40
20
0
HA
V1
V3
A2
F10
OA3
Gr29D09 Variants
Suppression
HR
*

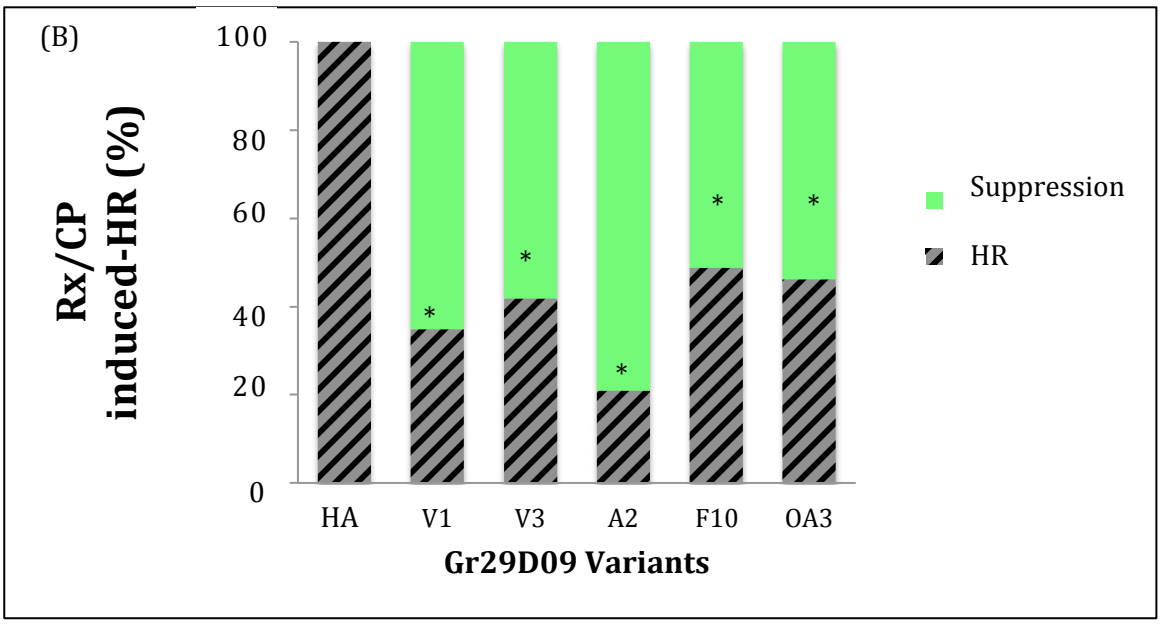
(B)
Rx/CP induced-HR (%)
100
80
60
40
20
0
HA
V1
V3
A2
F10
OA3
Gr29D09 Variants
Suppression
HR
*

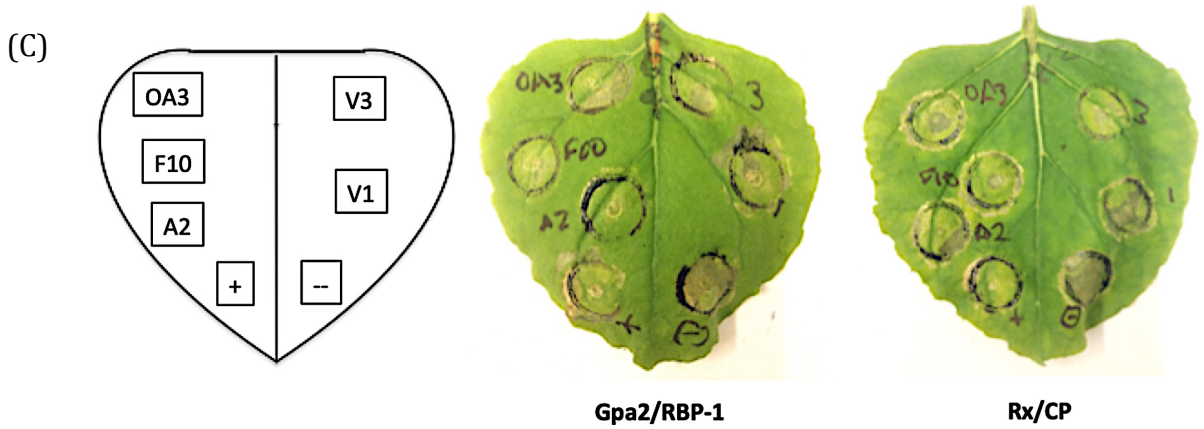

Fig. 3.2. Gr29D09 variants suppress cell death triggered by Gpa2/RBP-1 and Rx/CP in *Nicotiana benthamiana*. *Agrobacterium* cells carrying the *Gr29D09* expression constructs shown were infiltrated into *N. benthamiana* leaves 24 h prior to infiltration with *Agrobacterium* cells carrying Gpa2/RBP-1 (A) or Rx/CP (B, C). Constructs expressing the HA tag and *GrCEP12* (Chronis et al. 2013) were used as negative and positive controls, respectively. The hypersensitive response (HR) cell-death phenotype was scored 5 days after the last infiltration. The percent HR values shown on the y-axis are from ten and seven independent assays for Gpa2/RBP-1 and Rx/CP, respectively. Bars represent mean percentage HR for at least 39 leaf discs ($n \geq 39$) per replicate. (In Gpa2/RBP-1 assay, the total leaf disc numbers combining

from ten biological repeats for each variant are: V1: 62, V3: 75, A2: 67, F10: 67, OA3: 52. In Rx/CP assay, the total leaf disc numbers combining from seven biological repeats for each variant are: V1, V3, A2, F10: 43, OA3: 39) The asterisks indicate a significant difference between the empty vector and the tested variants (Student's t-test at $P< 0.05$). (C) Representative leaves from both Gpa2/RBP-1 and Rx/CP assays. The negative controls on both leaves had cell death over 75% of the agroinfiltration area and were regarded as HR response. The remaining leaf discs showed HR suppression. +, positive control. --, negative control. (D) Protein expression level of Gr29D09 variants in infiltrated *N. benthamiana* leaves. The leaf discs were collected 48 h after of agroinfiltration and subjected to Western Blotting.

Gr29D09-V3 physically interacts with StHXK7 *in planta*

In our laboratory, prior proteomic nanoLC-MS/MS analysis provided a list of host protein candidates that might interact with Gr29D09-V3 (Shiyan Chen, unpublished data). A subsequent co-immunoprecipitation (co-IP) assay found that StHXK7-Myc was pulled down with Gr29D09-V3$^{\Delta SP}$-HA but not with an StP69-HA control (Fig. 3.3A) and suggested that StHXK7 physically interacts with Gr29D09-V3. Though Gr29D09-V1, A2 and F10 showed interaction with StHXK7 with a co-IP assay (data not shown), Gr29D09-V3 exhibited the strongest suppression ability on ROS production and thus subsequent experiments focused on the interaction between Gr29D09-V3 and StHXK7. Intriguingly, microscopic examination showed distinct subcellular localization of Gr29D09-V3$^{\Delta SP}$ and StHXK7 when the green fluorescent protein (GFP) fusion proteins were transiently expressed in *N. benthamiana* (Fig. 3.3B). Gr29D09-V3$^{\Delta SP}$-GFP was previously identified as a cytoplasmic effector (Shiyan Chen, unpublished data; Fig 3.3B). In contrast, the colocalization with mitochondria marker AtCox4-mCherry (Mito-RFP) demonstrated StHXK7-GFP was mitochondria-associated (Fig. 3.3B).

To examine if Gr29D09-V3 and StHXK7 interact within plant cells, BiFC was conducted (Citovsky et al., 2006). Gr29D09-V3 and StHXK7 were fused to the N-terminal and C-terminal halves of yellow fluorescent protein (YFP) respectively. They were then co-expressed in *N. benthamiana* with agroinfiltration. The interaction between Gr29D09-V3 and StHXK7 reconstituted YFP signal on mitochondria in *N. benthamiana* epidermal cells (Fig. 3.3C). There was no fluorescent signal observed in the control experiment, which StHXK7-nYFP and Gr4G05-cYFP, a cytoplasmic nematode effector, were co-expressed in *N. benthamiana* (Fig. 3.3D). These BiFC results confirmed a specific interaction between Gr29D09-V3 and StHXK7 *in planta*, and reveal that the interaction may occur on the mitochondria of plant cells (Fig. 3.3C).

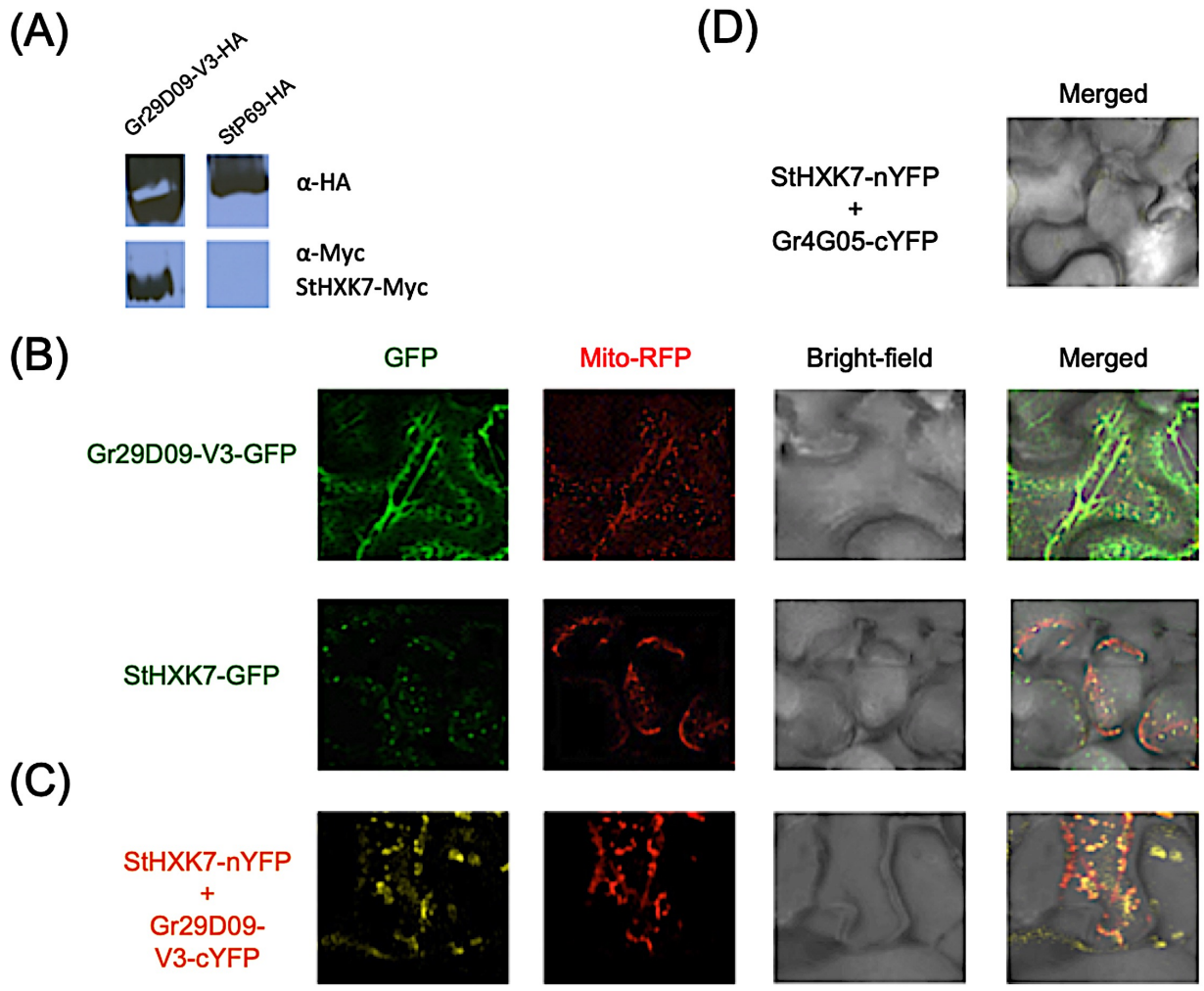

Fig. 3.3. StHXK7 is a potential host target of Gr29D09-V3. (A) Co-IP of protein extracts from agroinfiltrated leaves using anti-HA agarose beads confirmed that Myc-tagged StHXK7 associated specifically with Gr29D09-V3-HA and not with the StP69-HA control protein (Courtesy of Shiyan Chen). (B) *N. benthamiana* leaves were agroinfiltrated separately with Gr29D09-V3-GFP and StHXK7-GFP to determine the subcellular localization of Gr29D09-V3 and StHXK7 when expressed in the plant cell. (C) *N. benthamiana* leaves were co-transformed with StHXK7-nYFP-Myc and Gr29D09-V3-cYFP-HA.

BiFC revealed YFP signal and it colocalized with the mitochondria marker AtCox4-mCherry (Mito-RFP). (D) No YFP signal from the control *N. benthamiana* leaves with StHXK7-nYFP-Myc and Gr4G05-cYFP-HA co-infiltration. The bright-field images in (B-D) showed the epidermal cells in *N. benthamiana* leaves. The merged images combined signals from different channels to examine the colocalization. The images were taken 48 h after co-infiltration.

StHXK7 is up-regulated in nematode infection sites and its transcript abundance is influenced by *G. rostochiensis* and Gr29D09-V3

To investigate if the expression of *StHXK7* was affected in response to *G. rostochiensis* infection, wild-type potato plants were subjected to *G. rostochiensis* infection and the mRNA levels of *StHXK7* from roots at different dpi were quantified with RT-qPCR. The results revealed that *StHXK7* expression level was induced ~4-fold at 4 and 11 dpi in comparison with uninfected roots (Fig. 3.4A). To further examine whether the expression of *StHXK7* is directly impacted by Gr29D09-V3, the transcript level of *StHXK7* was also measured in roots of potato engineered to overexpress *Gr29D09-V3*; *StHXK7* levels were ~6-fold higher in the roots of *Gr29D09-V3* overexpression lines compared to levels in wild type potato (Fig. 3.4B). The spatial expression pattern of *StHXK7* was further examined using transgenic potato lines expressing a *StHXK7promoter:GUS* construct (Fig. 3.4C-I). In uninfected plants, GUS staining revealed *StHXK7* to be expressed in upper and lower sections of the stem, in leaf veins, and at the base of developed lateral roots (Fig. 3.4C-E). Following nematode infection, the expression of *StHXK7* was induced at and around nematode feeding sites during early and late nematode parasitic stages (Fig. 3.4F-I). Taken together, increased expression of

StHXK7 in nematode infection sites provides strong evidence of Gr29D09-V3-StHXK7 interaction confirmed by co-IP and BiFC. There was a possible feedback loop from Gr29D09-V3 to mediate the enhancement of *StHXK7* expression during nematode infection.

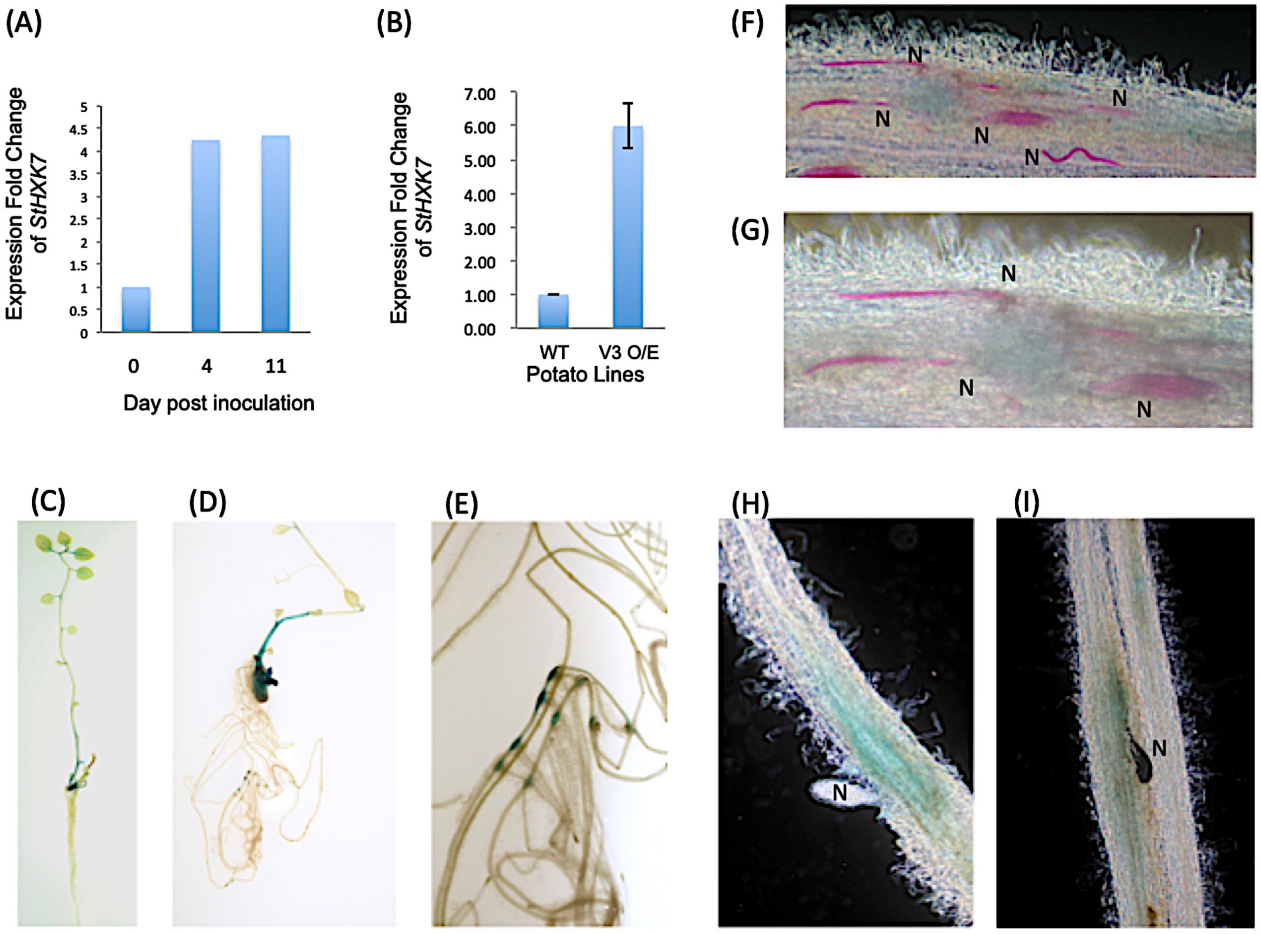

Fig. 3.4. Localization of *StHXK7* expression in potato plants with and without nematode infection.

(A) The expression profile of *StHXK7* in *G. rostochiensis*-infected potato roots was examined with RT-qPCR. The expression levels were first normalized to the housekeeping gene *StRPN7*. The fold change was then normalized to 0 dpi. This chart was from one experiment. The same trend of *StHXK7* upregulation was observed from two independent experiments. (B) The expression profile of *StHXK7* in roots of potato lines with *Gr29D09-V3* overexpression (V3 O/E) was examined with RT-qPCR. The fold

change is normalized to empty vector. The data are from two transgenic potato lines and normalized to wild type potato plants with empty vector (WT). (C) to (E) showed the histochemical localization of GUS activity indicating *StHXK7* expression in plant tissues. The GUS signals were found in the upper and lower parts of the stem (C, D), leaf veins, and at sites with developed lateral roots (E). (F) to (I), GUS activity indicating *StHXK7* expression in response to *G. rostochiensis* infection at early and later infection stages. GUS activity is observed at and around nematode infection sites. Acid fuchsine was used to stain nematode juveniles in red. Parasitic second- and third stage juveniles (par-J2 and par-J3) with 4X objective (F), 10X objective (G), par-J4 females (H and I). N, nematodes.

StHXK7 suppresses PTI response

As noted above, Gr29D09-V3 suppressed flg-22-triggered ROS production in *N. benthamiana.*, StHXK7 interacted with Gr29D09-V3 *in planta,* and its expression level was up-regulated at nematode feeding sites. These findings prompted me to investigate whether elevated expression of *StHXK7* is associated with inhibition of ROS generation. *A. tumefaciens* strain GV3101 carrying an *StHXK7-Myc* expression construct was infiltrated into *N. benthamiana* leaves and subjected to a luminol-based PTI assay with flg22 serving as an inducer. AvrPtoB and Myc tag-only vector were included as positive and negative controls. The luminol signal of the Myc tag-only vector was set to 100 and the signals from *AvrPtoB* and *StHXK7* infiltrated leaves were normalized to it. The potent PTI inhibitor AvrPtoB reduced ROS production by about 95%. StHXK7 also significantly interfered with ROS production, with maximum relative luminescence units reduced by ~80% (Fig3.5). These data reveal that StHXK7 can suppress ROS production.

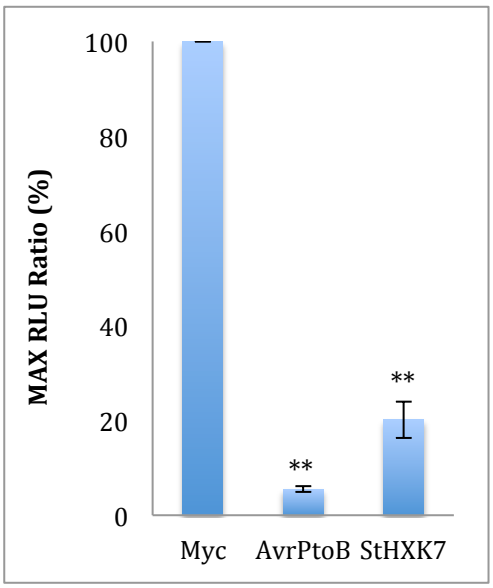

Fig. 3.5. StHXK7 suppresses flg22-triggered ROS production in *N. benthamiana.* *Agrobacterium tumefaciens* strain GV3101 carrying Myc, AvrPtoB and StHXK7 expression constructs were individually infiltrated into leaves of 3-week-old *N. benthamiana* plants. Infiltrated leaf discs were collected 48 h post-agroinfiltration and assayed for ROS production. Y-axis values indicate maximum relative luminescence units (MAX RLUs) ± SD of 21 leaf discs. The experiment was repeated twice and similar results were obtained each time. Significant differences from AvrPtoB and StHXK7 when compared to Myc are indicated by asterisks (Student's t-test at $P < 0.01$).

CHAPTER 4: DISCUSSION

In this thesis I presented evidence that one member, Gr29D09-V3, of the Gr29D09 effector family of *G. rostochiensis* physically interacts with StHXK7 *in planta*, and that the interaction is associated with mitochondria of plant cells. I further showed that *StHXK7* mRNA levels are elevated in *G. rostochiensis*-infected potato roots, in and around nematode feeding sites, and also in non-infected roots of potato lines overexpressing *Gr29D09-V3*. These findings of increased expression of *StHXK7* strongly support an interaction between Gr29D09-V3 and StHXK7 and it is likely modulated through a Gr29D09-V3-involved feedback loop during nematode parasitism. In a heterologous (*N. benthamiana)* system, transient expression of *StHXK7* resulted in suppression of ROS production triggered by flg22.

In eukaryotic cells, reactive oxygen species (ROS) are a group of highly reactive chemical molecules formed from reduction of O_2. Under normal conditions, ROS are natural by-products of cellular respiration and ROS-scavenging mechanisms are utilized to avoid detrimental stress from accumulating ROS inside cells. In contrast, when plants are challenged by pathogens, the immediate ROS burst is the hallmark of a plant immune response at an early stage of pathogen

invasion to prevent pathogen spread (Heath, 2000; Ali et al., 2018). Studies have shown that plant-parasitic nematodes have evolved strategies to safeguard themselves from ROS produced by host plants. Plant-parasitic nematodes encode antioxidant proteins, such as superoxide dismutase, catalase (Molinari and Miacola, 1997; Solo et al., 2021) and GpX (Jones et al., 2004) that may function in detoxifying ROS produced by host plant cells. Plant-parasitic nematodes also utilize effectors to reduce cellular damage caused by ROS, e.g. 10A06 secreted by *H. schachtii* interacts with *Arabidopsis* spermidine synthase to activate a set of antioxidant genes in plants (Hewezi et al., 2010).

The data presented in this thesis represent the first time that a plant hexokinase (StHXK7) was shown to interact with a pathogenic effector to dampen the host immune response. Hexokinases are well known to be responsible for the first step of glycolysis. Even so, accumulating studies across different eukaryotes have shown that hexokinases also play a role in ROS-scavenging. Knocking down Hexokinase-II in mice led to increased cellular ROS production (Wu et al., 2012), while overexpression of *Arabidopsis HXK1* and *HXK2* enhanced ability to resist cell death caused by exogenous H_2O_2 treatment in protoplasts (Kim et al., 2006)

and activation of hexokinase in potato tubers, under normal conditions, reduced H_2O_2 release (Camacho-Pereira et al., 2008).

The finding that StHXK7 is a host interactor of Gr29D09-V3 makes StHXK7 a potential target for disease management. There are two potential applications. One is through engineering disease-resistant potatoes and the other is removing StHXK7 from mitochondria. Susceptibility genes (S-genes) in plants play roles in promoting pathogenesis and perturbing S-gene's functions could enhance disease resistance of plants (Zaidi et al., 2020). For example, knocking out selected S-genes by CRISPR/Cas9 technology increased resistance against late blight in potatoes (Kieu et al., 2021). Since the presence of StHXK7 facilitates nematode parasitism, *StHXK7* is a potential susceptibility gene. It may be possible to generate potatoes with enhanced resistance against *G. rostochiensis* through CRISPR/Cas9-targeted mutagenesis of *StHXK7*. If the engineered potatoes grow as well as wild type and show reduced susceptibility to nematode infection, such engineered potatoes could be used to manage nematode infection.

Unbound hexokinase proteins are degraded quickly through the ubiquitin pathway when compared to hexokinases bound to mitochondria (Magnani et al., 1992; Okatsu et al., 2012). This

has made human mitochondria associated Hexokinase-II (HKII) an attractive anti-cancer target, as HK-II promotes tumor growth (Krasnov et al., 2013). Deploying molecules such as 3-bromopyruvate (3-BrPA) (which interferes with hexokinase function) and the N-terminal 15 amino acids of HKII (N-HK II peptide) (which translocates mitochondria-bound hexokinases to the cytoplasm) are two anti-cancer strategies (Chen et al., 2009; Bryan and Raisch, 2015). Comparable strategies could be tested in potatoes to interfere with cyst nematode infection. Chemical compounds such as 3-BrPA may have ability to inhibit StHXK7 in plants. Since neither HK-II-3-BrPA nor StHXK7 have crystal structure information, *in silico* structure prediction could be used to first screen potential chemical inhibitors. The chemical inhibitor candidates could then be tested in a PTI assay with *Gr29D09-V3* infiltrated in tobacco leaves to evaluate if Gr29D09-V3 loses the ability to suppress ROS production. Similarly, StHXK7 without the N-terminal mitochondria anchor could be examined to see if it loses the ability to inhibit ROS in PTI assays. If so, the N-terminal mitochondria anchor of StHXK7 could be utilized in a PTI assay. Through competing the space on mitochondria with full length StHXK7, the N-terminal mitochondria anchor of StHXK7 could possibly translocate full length one to the

cytoplasm. Whether Gr29D09-V3 shows reduced ability of inhibiting ROS production could be examined by co-infiltrating *Gr29D09-V3* and the N-terminal mitochondria anchor of *StHXK7* into tobacco leaves followed by PTI assay.

Among 27 known Gr29D09 variants, five were selected for functional characterization in this thesis. Gr29D09-V3 exhibited the strongest ROS suppression ability in PTI assays while Gr29D09-A2 showed the strongest inhibition of HR in ETI assays. This may indicate that these two variants target different host proteins. One way to identify the host target of Gr29D09-A2 would be through interactome screening with Co-IP and nanoLC-MS/MS analysis.

Our laboratory previously found the frequency of Gr29D09-V3 was 40% higher in Ro2, a pathotype of *G. rostochiensis* that overcomes the *H1* resistance gene, when compared to the avirulent Ro1 pathotype (Tran, 2016), suggesting that Gr29D09-V3 may play a role in overcoming *H1*.

Collectively, the data in this thesis suggest that the Gr29D09 family evolved to interfere with different components of plant defense pathways. The specific defense suppression described in this thesis surrounds Gr29D09-V3 inhibiting ROS production through interaction with the host

protein StHXK7.

REFERENCES

Akker, den, S.E.-V., Laetsch, D.R., Thorpe, P., Lilley, C.J., Danchin, E.G.J., Rocha, M.D., Rancurel, C., Holroyd, N.E., Cotton, J.A., Szitenberg, A., Grenier, E., Montarry, J., Mimee, B., Duceppe, M-O., Boyes, I, Marvin, J. M.C., Jones, L.M., Yusup, H.B., Lafond-Lapalme, J., Esquibet, M., Sabeh, M., Rott, M., Overmars, H., Finkers-Tomczak, A., Smant, G., Koutsovoulos, G., Blok, V., Mantelin, S., Cock, P.J., Phillips, W., Henrissat, B., Urwin, P.E., Blaxter, M., and Jones, J.T. (2017). The genome of the yellow potato cyst nematode, Globodera rostochiensis, reveals insights into the basis of parasitism and virulence. Genome Biology 17: 1–23.

Ali, M.A., Anjam, M.S., Nawaz, M.A., Lam, H.-M., and Chung, G. (2018). Signal Transduction in Plant–Nematode Interactions. International Journal of Molecular Sciences 2019, Vol. 20, Page 5360 19: 1648.

Bendahmane, A., Querci, M., Kanyuka, K., and Baulcombe, D.C. (2000). Agrobacterium transient expression system as a tool for the isolation of disease resistance genes: application to the Rx2 locus in potato. Plant J. 21: 73–81.

Boller, T. and Felix, G. (2009). A renaissance of elicitors: perception of microbe-associated molecular patterns and danger signals by pattern-recognition receptors. Annu Rev Plant Biol 60: 379–406.

Bryan, N. and Raisch, K. (2015). Identification of a Mitochondrial-Binding Site on the Amino-Terminal End of Hexokinase II. Biosci. Rep.: 1–7.

Camacho-Pereira, J., Meyer, L.E., Machado, L.B., Oliveira, M.F., and Galina, A. (2008). Reactive Oxygen Species Production by Potato Tuber Mitochondria Is Modulated by Mitochondrially Bound Hexokinase Activity. Plant Physiol. 149: 1099–1110.

Chen, S., Chronis, D., and Wang, X. (2013). The novel GrCEP12 peptide from the plant-parasitic nematode Globodera rostochiensis suppresses flg22-mediated PTI. Plant Signal Behav 8: e25359.

Chen, Z., Zhang, H., Lu, W., and Huang, P. (2009). Role of mitochondria-associated hexokinase II in cancer cell death induced by 3-bromopyruvate. Biochim Biophys Acta 1787: 553–560.

Chitwood, D.J. (2003). Research on plant-parasitic nematode biology conducted by the United States Department of Agriculture-Agricultural Research Service. Pest Manag Sci 59: 748–753.

Chronis, D., Chen, S., Lang, P., Tran, T., Thurston, D., and Wang, X. (2014a). In vitro Nematode Infection on Potato Plant. Bio-protocol 4: 1–9.

Chronis, D., Chen, S., Lang, P., Tran, T., Thurston, D., and Wang, X. (2014b). Potato Transformation. Bio-protocol 4: e1017–e1017.

Chronis, D., Chen, S., Lu, S., Hewezi, T., Carpenter, S.C.D., Loria, R., Baum, T.J., and Wang, X. (2013). A ubiquitin carboxyl extension protein secreted from a plant-parasitic nematode Globodera rostochiensis is cleaved in planta to promote plant parasitism. Plant J. 74: 185–196.

Citovsky, V., Lee, L.-Y., Vyas, S., Glick, E., Chen, M.-H., Vainstein, A., Gafni, Y., Gelvin, S.B., and Tzfira, T. (2006). Subcellular localization of interacting proteins by bimolecular fluorescence complementation in planta. J Mol Biol 362: 1120–1131.

Cotton, J.A., Lilley, C.J., Jones, L.M., Kikuchi, T., Reid, A.J., Thorpe, P., Tsai, I. J., Beasley, H., Blok, V., Cock, P.J., Akker, den, S.E-V, Holroyd, N., Hunt, M., Mantelin, S., Naghra, H., Pain, A., Palomares-Rius, J. E., Zarowiecki, M., Berriman, M., Jones, J.T., Urwin, P.E. (2014). The genome and life-stage specific transcriptomes of Globodera pallida elucidate key aspects of plant parasitism by a cyst nematode. Genome Biology 15: R43.

Gao, B., Allen, R., Maier, T., Davis, E.L., Baum, T.J., and Hussey, R.S. (2007). The Parasitome of the Phytonematode Heterodera glycines. Mol. Plant Microbe Interact. 16: 720–726.

Gheysen, G. and Mitchum, M.G. (2011). How nematodes manipulate plant development pathways for infection. Curr. Opin. Plant Biol. 14: 415–421.

Heath, M.C. (2000). Hypersensitive response-related death. Plant Mol Biol 44: 321–334.

Hewezi, T., Howe, P.J., Maier, T.R., Hussey, R.S., Mitchum, M.G., Davis, E.L., and Baum, T.J. (2010). Arabidopsis Spermidine Synthase Is Targeted by an Effector Protein of the Cyst Nematode Heterodera schachtii. Plant Physiol. 152: 968–984.

Hogenhout, S.A., van der Hoorn, R.A.L., Terauchi, R., and Kamoun, S. (2009). Emerging concepts in effector biology of plant-associated organisms. Mol. Plant Microbe Interact. 22: 115–122.

Hussey, R.S. (1989). Disease-Inducing Secretions of Plant-Parasitic Nematodes. Annu Rev Phytopathol 27: 123–141.

Hussey, R.S. and Mims, C.W. (1991). Ultrastructure of feeding tubes formed in giant-cells induced in plants by the root-knot nematodeMeloidogyne incognita. Protoplasma 162: 99–107.

Jefferson, R.A., Kavanagh, T.A., and Bevan, M.W. (1987). GUS fusions: beta-glucuronidase as a sensitive and versatile gene fusion marker in higher plants. The EMBO Journal 6: 3901–3907.

Jones, J.D.G. and Dangl, J.L. (2006). The plant immune system. Nature 444: 323–329.

Jones, J.T., Haegeman, A., Danchin, E.G.J., Gaur, H.S., Helder, J., Jones, M.G.K., Kikuchi, T., Manzanilla-López, R., Palomares-Rius, J.E., Wesemael, W.M.L., and Perry, R.N. (2013). Top 10 plant-parasitic nematodes in molecular plant pathology. Mol. Plant Pathol. 14: 946–961.

Jones, J.T., Kumar, A., Pylypenko, L.A., Thirugnanasambandam, A., Castelli, L., Chapman, S., Cock, P.J.A., Grenier, E., Lilley, C.J., Phillips, M.S., and Blok, V.C. (2009). Identification

and functional characterization of effectors in expressed sequence tags from various life cycle stages of the potato cyst nematode Globodera pallida. Mol. Plant Pathol. 10: 815–828.

Jones, J.T., Reavy, B., Smant, G., and Prior, A.E. (2004). Glutathione peroxidases of the potato cyst nematode Globodera Rostochiensis. Gene 324: 47–54.

Keppler, L.D., Baker, C.J., and Atkinson, M.M. (1989). Active oxygen production during a bacteria-induced hypersensitive reaction in tobacco suspension cells. Phytopathology: 974–978.

Kieu, N.P., Lenman, M., Wang, E.S., Petersen, B.L., and Andreasson, E. (2021). Mutations introduced in susceptibility genes through CRISPR/Cas9 genome editing confer increased late blight resistance in potatoes. Sci Rep: 1–12.

Kim, M., Lim, J.-H., Ahn, C.S., Park, K., Kim, G.T., Kim, W.T., and Pai, H.-S. (2006). Mitochondria-associated hexokinases play a role in the control of programmed cell death in Nicotiana benthamiana. Plant Cell 18: 2341–2355.

Kim, Y.J., Lin, N.C., and Martin, G.B. (2002). Two distinct Pseudomonas effector proteins interact with the Pto kinase and activate plant immunity. Cell 109: 589–598.

Krasnov, G.S., Dmitriev, A.A., Lakunina, V.A., Kirpiy, A.A., and Kudryavtseva, A.V. (2013). Targeting VDAC-bound hexokinase II: a promising approach for concomitant anti-cancer therapy. Expert Opin Ther Targets 17: 1221–1233.

Lindeberg, M., Cunnac, S., and Collmer, A. (2012). Pseudomonas syringae type III effector repertoires: last words in endless arguments. Trends Microbiol 20: 199–208.

Lu, S.-W., Chen, S., Wang, J., Yu, H., Chronis, D., Mitchum, M.G., and Wang, X. (2009). Structural and functional diversity of CLAVATA3/ESR (CLE)-like genes from the potato cyst nematode Globodera rostochiensis. Mol. Plant Microbe Interact. 22: 1128–1142.

Lu, S.-W., Tian, D., Borchardt-Wier, H.B., and Wang, X. (2008). Alternative splicing: a novel mechanism of regulation identified in the chorismate mutase gene of the potato cyst nematode Globodera rostochiensis. Mol Biochem Parasitol 162: 1–15.

Lu, Y. and Tsuda, K. (2021). Intimate Association of PRR- and NLR-Mediated Signaling in Plant Immunity. Molecular Plant-Microbe Interactions® 34: 3–14.

Luna, E., Pastor, V., Robert, J., Flors, V., Mauch-Mani, B., and Ton, J. (2011). Callose deposition: a multifaceted plant defense response. Mol. Plant Microbe Interact. 24: 183–193.

Magnani, M., Crinelli, R., Corsi, D., and Serafini, G. (1992). Intracellular distribution of protein as a determinant for ubiquitination and proteolytic degradation. Ann N Y Acad Sci 673: 103–109.

Mitchum, M.G., Hussey, R.S., Baum, T.J., Wang, X., Elling, A.A., Wubben, M., and Davis, E.L. (2013). Nematode effector proteins: an emerging paradigm of parasitism. New Phytol. 199: 879–894.

Molinari, S. and Miacola, C. (1997). Antioxidant enzymes in phytoparasitic nematodes. Journal of Nematology 29: 153–159.

Okatsu, K., Iemura, S.-I., Koyano, F., Go, E., Kimura, M., Natsume, T., Tanaka, K., and Matsuda, N. (2012). Mitochondrial hexokinase HKI is a novel substrate of the Parkin ubiquitin ligase. Biochemical and Biophysical Research Communications 428: 197–202.

Peng, Y., van Wersch, R., and Zhang, Y. (2018). Convergent and Divergent Signaling in PAMP-Triggered Immunity and Effector-Triggered Immunity. Molecular Plant-Microbe Interactions® 31: 403–409.

Sacco, M.A., Koropacka, K., Grenier, E., Jaubert, M.J., Blanchard, A., Goverse, A., Smant, G., and Moffett, P. (2009). The cyst nematode SPRYSEC protein RBP-1 elicits Gpa2- and RanGAP2-dependent plant cell death. PLoS Pathogens 5: e1000564.

Saijo, Y., Loo, E.P.-I., and Yasuda, S. (2018). Pattern recognition receptors and signaling in plant-microbe interactions. Plant J. 93: 592–613.

Segonzac, C., Feike, D., Gimenez-Ibanez, S., Hann, D.R., Zipfel, C., and Rathjen, J.P. (2011). Hierarchy and roles of pathogen-associated molecular pattern-induced responses in Nicotiana benthamiana. Plant Physiol. 156: 687–699.

Smant, G., Stokkermans, J.P., Yan, Y., Boer, de, J.M., Baum, T.J., Wang, X., Hussey, R.S., Gommers, F.J., Henrissat, B., Davis, E.L., Helder, J., Schots, and A., Bakker, J. (1998). Endogenous cellulases in animals: Isolation of β-1,4-endoglucanase genes from two species of plant-parasitic cyst nematodes. Proc. Natl. Acad. Sci. U.S.A. 95: 4906–4911.

Solo, N., Kud, J., Caplan, A., Kuhl, J., Xiao, F., and Dandurand, L.-M. (2021). Characterization of the superoxide dismutase (SOD) from the potato cyst nematode, Globodera pallida. Phytopathology.

Thorpe, P., Mantelin, S., Cock, P.J., Blok, V.C., Coke, M.C., Akker, den, S.E.-V., Guzeeva, E., Lilley, C.J., Smant, G., Reid, A.J., Wright, K.M., Urwin, P.E., and Jones, J.T. (2014). Genomic characterisation of the effector complement of the potato cyst nematode Globodera pallida. BMC Genomics 15: 923.

Tran, T. (2016). The Novel Gr29D09 Effector Family From Potato Cyst Nematode Globodera Rostochiensis Suppresses Plant Immunity To Promote Nematode Parasitism. PhD thesis, Cornell University, Ithaca

Vieira, P. and Gleason, C. (2019). Plant-parasitic nematode effectors - insights into their diversity and new tools for their identification. Curr. Opin. Plant Biol. 50: 37–43.

Wu, R., Wyatt, E., Chawla, K., Tran, M., Ghanefar, M., Laakso, M., Epting, C.L., and Ardehali, H. (2012). Hexokinase II knockdown results in exaggerated cardiac hypertrophy via increased ROS production. EMBO Mol Med 4: 633–646.

Yang, S., Pan, L., Chen, Y., Yang, D., Liu, Q., and Jian, H. (2019). Heterodera avenae GLAND5 Effector Interacts With Pyruvate Dehydrogenase Subunit of Plant to Promote Nematode Parasitism. Front Microbiol 10: 1241.

Zaidi, S.S.-E.-A., Mahas, A., Vanderschuren, H., and Mahfouz, M.M. (2020). Engineering crops of the future: CRISPR approaches to develop climate-resilient and disease-resistant plants.: 1–19.